

Formation and characterization of oxynitride glasses in the Si-Ca-Al-O-N and Si-Ca-Al,B-O-N systems

PAUL E. JANKOWSKI*, SUBHASH H. RISBUD

Department of Ceramic Engineering and Materials Research Laboratory, University of Illinois at Urbana-Champaign, Urbana, IL 61801, USA

Oxynitride compositions in the Si-Ca-Al-O-N and Si-Ca-Al, B-O-N systems were melted and furnace-cooled in BN crucibles at temperatures from ≈ 1650 to 1850°C under dry nitrogen atmospheres. Glass formation, phase stability and crystallization were studied by characterizing the cooled melts by X-ray diffraction, DTA, and electron microscopy. Oxynitride batches with nitrogen content up to ≈ 11 at % formed glasses in the Si-Ca-Al-O-N system. Glasses in the Si-Ca-Al, B-O-N system could be formed only when the B_2O_3 content of the batch was less than ≈ 3 wt %. Oxynitride glasses in these boron-containing systems were characteristically inhomogeneous, difficult to process, and prone to crystallization. In both the systems, glasses exhibited glass transitions beginning at $\approx 1000^\circ\text{C}$ and crystallization at ≈ 1300 to 1500°C . Nitrogen-containing crystalline phases were identified in devitrified glasses via microstructural and micro-mechanical analyses.

1. Introduction

Burgeoning interest in nitrogen ceramics in the last two decades has resulted in considerable efforts being directed towards the fabrication and properties of Si_3N_4 and several multicomponent materials in Si-metal-O-N systems. One of the many fascinating aspects of these developments is the growing enthusiasm for investigating a new set of non-crystalline materials generally referred to as oxynitride glasses [1-15].

In the present work we have investigated glass formation and stability in the oxynitride systems Si-Ca-Al-O-N and Si-Ca-Al, B-O-N. The goals were to obtain and characterize glasses in these systems with respect to thermal stability, crystallization, and microstructure.

2. Experimental procedures

2.1. Materials synthesis

Appropriately batched oxide and nitride ceramic powders were charged into BN crucibles (≈ 2.5

cm diameter \times 5 cm height) and lightly pressed. The crucible was jacketed by a graphite sleeve and the assembly loaded into the chamber of a high temperature graphite element furnace[†] capable of operating up to $\approx 2500^\circ\text{C}$. A schematic sketch of the furnace and the experimental set-up used is shown in Fig. 1. Crucibles were heated in the furnace at $\approx 30^\circ\text{C min}^{-1}$ under an atmosphere of dry nitrogen (flow rate $\approx 500\text{ cm}^3\text{ min}^{-1}$) until the melt processing temperature (≈ 1650 , 1750 or 1850°C) was reached. Following a 7 h soak at this temperature, the furnace was shut off and allowed to cool. The average cooling rate of the crucible was $32^\circ\text{C min}^{-1}$ down to 800°C , at which time the crucible was removed and quenched in water. Some melts were lowered into a nitrogen glove box and allowed to cool in flowing nitrogen.

2.2. Materials characterization

Materials were characterized by differential

*Now at Corning Glass Works, Corning, New York 14830, USA.

[†]Model 1000A, Astro Industries Inc., Santa Barbara, California, USA.

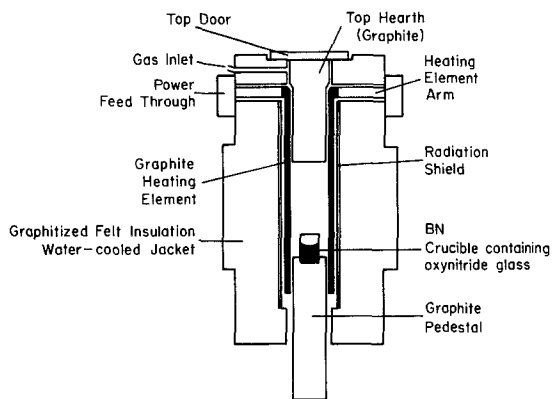


Figure 1 Schematic sketch of the high temperature graphite element furnace used for preparation of oxynitride glasses.

thermal analysis (DTA)* using ≈ 10 mg powdered samples contained in alumina sample cups. DTA traces were obtained in a flowing nitrogen atmosphere at a heating rate of $10^\circ \text{C min}^{-1}$.

X-ray diffraction data were obtained on crushed powdered samples at a scan rate of 1°min^{-1} . Scanning electron microscopy (SEM) and energy dispersive X-ray analysis[†] were conducted on freshly fractured surfaces. SEM images were obtained after etching in a 48% HF acid solution for 15 sec. A thin film of gold was evaporated on the surfaces to reduce charging by the electron beam.

3. Results and discussion

3.1. Melt processing and glass formation

Tables I and II list some of the batch compositions studied for glass formation in the Si–Ca–Al–O–N and Si–Ca–Al, B–O–N systems. It is evident that the batch powders are refractory materials with high melting points. SiO_2 and Al_2O_3 have melting points of ≈ 1720 and 2050°C respectively. Cal-

cium nitride, Ca_3N_2 , forms a stable liquid at 1200°C and is an excellent solvent for aluminium nitride, which does not melt under normal conditions. Processing temperatures of the batches were chosen experimentally in the range ≈ 1650 to 1850°C . When processed at 1650°C , the batch fused, leaving a porous crystalline mass. When exposed to water, particular regions decomposed, suggesting that pockets of unreacted nitride existed in the mass. When soaked at 1850°C , the powders melted, and when cooled slowly, resulted in a glass. However, extreme volatilization had occurred during this soak, as evidenced by deposits in the cooler regions of the furnace and the small amount of materials left in the crucible. At 1750°C glasses were obtained without excessive volatilization losses, and these compositions are shown in Tables I and II. The BN crucibles are apparently unreactive with the melts since the melt/crucible interface was usually sharp and clean. The glass ingots did adhere to the crucible walls, but usually could be removed by tapping. Si–Ca–Al–O–N glasses were obtained from batches with SiO_2 contents from ≈ 72 to 80 wt%, as shown in Table I. Glasses in this system could not be formed, under the present experimental conditions, when the SiO_2 in the batch was < 50 wt% or > 80 wt%. The influence of boron on the glass-forming tendency was determined by melting B_2O_3 containing batches (Table II). Glasses formed only when the B_2O_3 content was below approximately 3 wt% but these glasses were often macroscopically inhomogeneous. As the boric anhydride addition increased, the temperature required to melt the batch increased. At approximately 25 wt% B_2O_3 the temperature required to obtain complete melting exceeded 2050°C . At this temperature volatilization losses were extraordinary and devitrification

TABLE I Si–CaAlON compositions

Sample number	Composition (wt%) as-batched					Nitrogen content (at %)	X-ray diffraction identification
	SiO_2	Al_2O_3	CaO	Ca_3N_2	AlN		
1	58.5	33.2	–	8.0	–	≈ 2.0	Glass
2	60.0	23.6	–	8.2	8.2	≈ 6.5	Glass
3	72.0	8.0	–	10.0	10.0	≈ 7.9	Glass
4	72.1	–	11.4	–	16.5	≈ 8.5	Glass
5	73.1	–	–	10.2	16.7	≈ 11.2	Glass
6	62.1	–	9.7	–	28.2	≈ 13.5	Crystalline
7	62.9	–	–	8.6	28.5	≈ 17.0	Crystalline

*Dupont Model 1090 DTA with 1091 Microprocessor, E. I. Dupont de Nemours, Inc., Wilmington, Delaware, USA.

†JEOL JSM-35C-SEM and Model 595 Scanning Auger Microprobe System (Physical Electronics Industries), Materials Research Laboratory, University of Illinois, Urbana, USA.

TABLE II Si-CaAlBON compositions

Sample number	Composition (wt %) as-batched					Nitrogen content (at %)	X-ray diffraction identification
	SiO ₂	B ₂ O ₃	Al ₂ O ₃	Ca ₃ N ₂	AlN		
8	81.1	3.1	4.5	11.3	—	3.1	Glass
9	74.4	2.8	4.2	10.3	8.3	7.0	Glass
10	73.0	2.8	4.1	10.1	10.1	8.0	Glass
11	50.3	12.6	—	8.6	28.5	16.0	Crystalline
12	36.0	24.0	23.6	8.2	8.2	6.5	Crystalline

was unavoidable with our experimental procedure. The maximum batched nitrogen content in the oxynitride glasses studied was ≈ 11 at % for a glass in the Si-Ca-Al-O-N system and ≈ 8 at % for a glass in the Si-Ca-(Al, B)-O-N system (Tables I and II). Chemical analyses conducted on selected samples from these systems and other metal-SiAlON glasses prepared in our laboratory using the same procedure have usually shown that about 60 to 70% of the batched nitrogen is retained in glasses melted at 1700 to 1750°C. It is therefore estimated that the maximum values of analysed nitrogen in the samples shown in Tables I and II are ≈ 5 at % for the Si-Ca-Al, B-O-N glasses and ≈ 7 at % for the Si-CaAlON glasses.

3.2. Thermal analysis (DTA)

Fig. 2 shows representative DTA curves obtained for three glasses. Note that the composition was such that only the nitrogen to oxygen ratio is changed while the calcium, silicon and aluminium concentrations remain the same in these glasses ($\text{Ca}_{3.4}\text{Si}_{20.2}\text{Al}_{13.5}\text{O}_y\text{N}_x$). In a number of samples

the DTA traces showed multiple peaks (both exothermic and endothermic) and the onset of the first endotherm during heating was taken to be the glass transition temperature (T_g) while the first exotherm was taken to be the crystallization temperature (T_c). The T_g and T_c values thus obtained are shown in Table III. The trend toward increasing T_g with higher nitrogen content can be seen in Si-Ca-Al-O-N glasses but similar behaviour in the Si-CaAlBON system cannot be easily discerned from the data; this could be due to the inhomogeneity of the boron-containing glasses. The increase in T_g with nitrogen content has been shown to occur in several Si-M-Al-O-N glasses (where M = yttrium, neodymium, calcium and magnesium) by Drew *et al.* [10], in Si-Y-Al-O-N glasses by Loehman [5] and in a recent study on Si-Ba-Al-O-N glasses by Tredway and Risbud [15]. The T_g values obtained for Si-CaAlON glasses (≈ 1000 to 1080°C) in the present study are higher than the T_g data reported by Drew *et al.* [10] (≈ 825 to 900°C) and could be attributed to differences in the Ca:Al:Si ratios in the two studies. Drew *et al.* [10] studied $\text{Ca}_{18}\text{Si}_{18}\text{Al}_6\text{O}_y\text{N}_x$ glasses while our glasses were based on $\text{Ca}_{3.4}\text{Si}_{20.2}\text{Al}_{13.5}\text{O}_y\text{N}_x$ compositions.

Fig. 2 also shows increases in the values of T_c with nitrogen content and while an increase is observed in some cases, the multiple T_c peaks

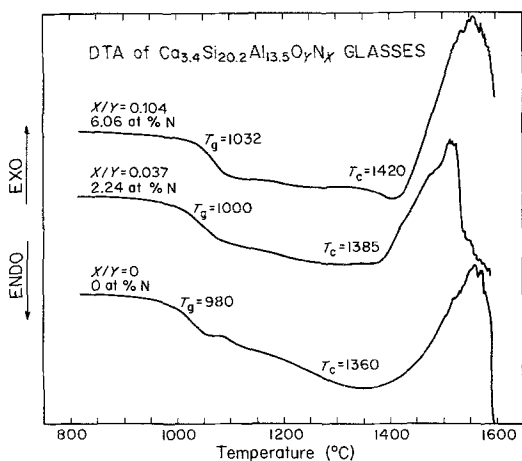


Figure 2 Typical DTA traces obtained during heating of Si-Ca-Al-O-N glasses at a heating rate of 10°C min⁻¹. Note the increase in glass transition and crystallization temperatures with increasing nitrogen content in the glass.

TABLE III Glass transition (T_g) and crystallization (T_c) temperatures of Si-CaAlON and Si-CaAlBON glasses

Sample number*	Nitrogen content (at %)	T_g (°C)	T_c (°C)
	0	998	1320
1	2.0	1000	1380
2	6.5	1032	1420
3	7.9	1080	1445
4	8.5	1080	1408
8	3.1	935	1440
9	7.0	1060	1443
10	8.0	975	1352

*Refer to Tables I and II.

make it difficult to establish a definite trend. Nevertheless, the T_c values are usually near $\approx 1400^\circ\text{C}$ for oxynitride glasses of both systems studied in this work. These are higher by $\approx 300^\circ\text{C}$ in comparison with the T_c values reported by Drew *et al.* [10].

3.3. Microscopy

Si–CaAlON glasses were generally homogeneous although phase separation was observed after heat treatment. Si–CaAlBON glasses were, however, quite inhomogeneous and often showed macroscopic segregation of metallic particles. Fig. 3 shows a micrograph of a polished cross-section of a glass (Sample 9, Table II) in the Si–Ca–AlBON system. Extensive inhomogeneity was evident in this sample, including regions of dark blue-grey colouration and some faint brown regions in the centre of the melt. Cracks developed during cooling can also be seen in Fig. 3.

The macroscopic droplet formation ($\approx 0.2\text{ cm}$ across), marked 3 in Fig. 3, and other adjacent areas of the sample were analysed by SEM to determine microchemistry. Fig. 4 shows elemental maps of silicon, calcium and aluminium obtained in the vicinity of the droplet region marked 3. The droplet is virtually all silicon and significant silicon

concentrations can also be observed in adjacent areas of the sample. Integrated intensities of silicon, calcium and aluminium were obtained at regions marked 1, 2 and 3 in Fig. 3 so that estimates of concentrations at various depths in the melt could be obtained. The calcium concentration showed an increase with melt depth and this behaviour was found along the centre and edges of the crucibles as shown in Fig. 5. Similar analyses showed that the silicon and aluminium concentrations decreased with melt depth (Fig. 5).

3.4. Phase separation and crystallization

Heat treated glasses were examined by X-ray diffraction and electron microscopy to characterize the microstructure and phase development. Table IV summarizes the X-ray diffraction data on selected heat treated samples all of which were heated at 1350°C for 2 h in the graphite furnace and cooled at normal rates. Fig. 6 is an SEM micrograph showing amorphous phase separation developed in a Si–CaAlON glass with $\approx 7.9\%$ batched nitrogen (Sample 3, Table I). The size of the separation ranges from 2.88 to $14.4\ \mu\text{m}$. The majority of the phase separated droplets are of the order of $5.76\ \mu\text{m}$. The relatively uniform phase distribution suggests that these glasses

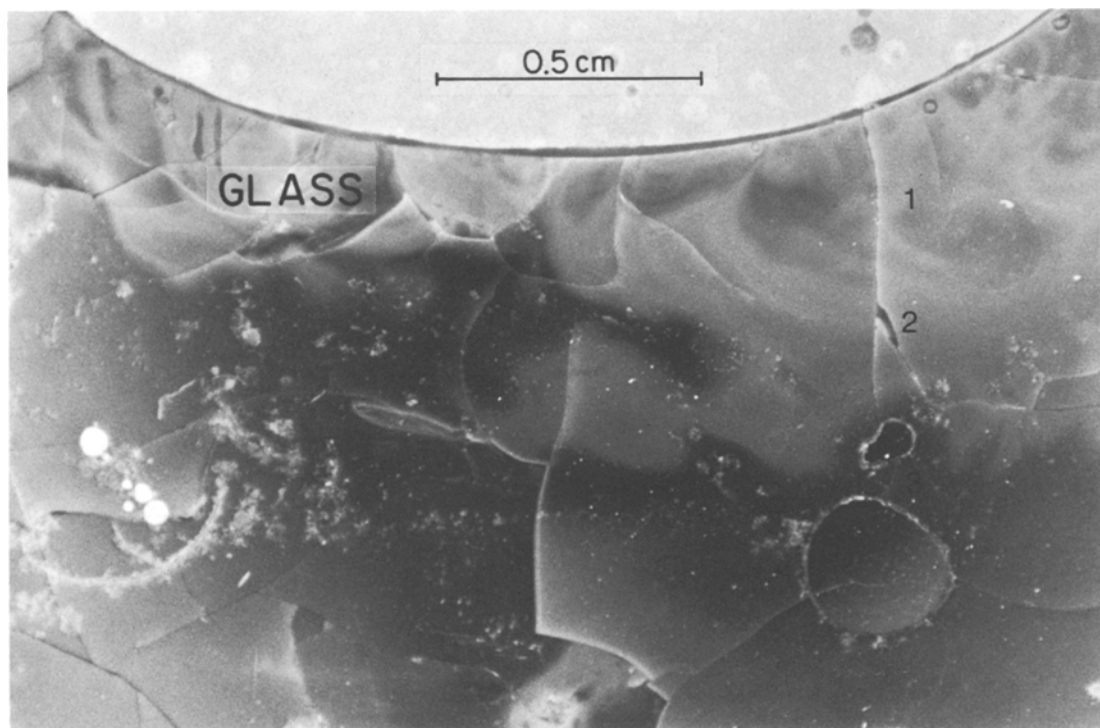


Figure 3 Micrograph of a cross-section of an inhomogeneous oxynitride glass in the Si–Ca–Al, B–O–N system.

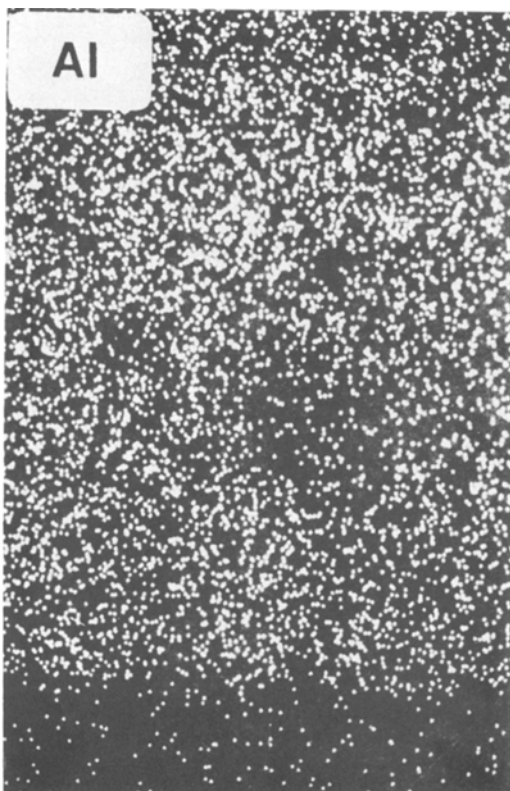
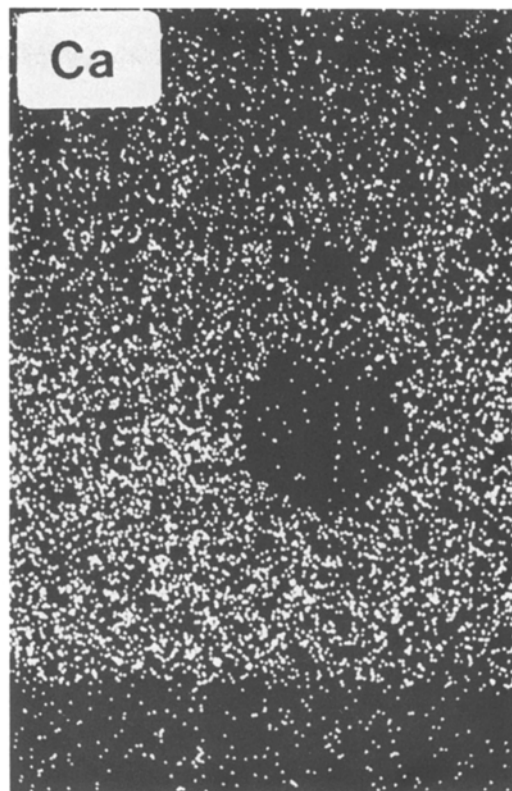
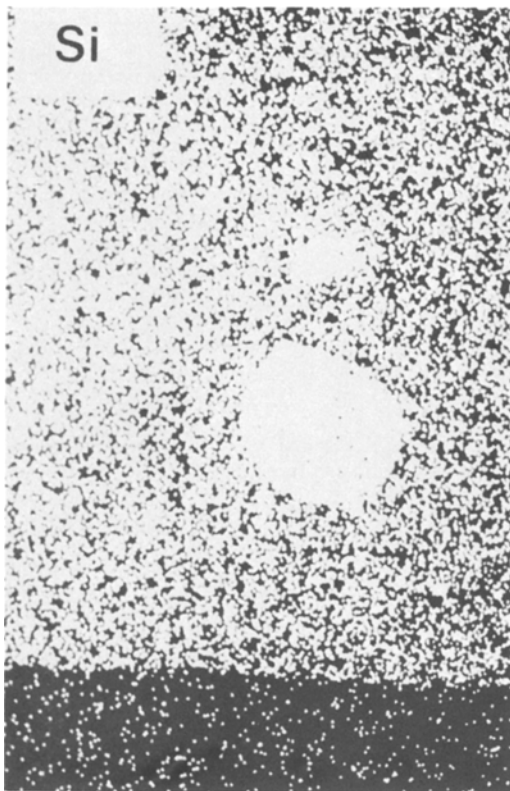


Figure 4 Elemental maps for silicon, calcium and aluminum obtained in the vicinity of the region marked 3 in Fig. 3.

might be suitable for the development of glass-ceramics.

Fig. 7 shows the microstructure and microchemistry of a crystallized Si-CaAlON sample with ≈ 8.5 at % nitrogen (Sample 4, Table I). X-ray identification had shown the presence of $\text{Si}_2\text{N}_2\text{O}$ crystallites in this sample. When analysed by X-ray energy dispersive spectrometry (EDS) in a scanning auger microprobe the crystalline area of the sample (Fig. 7) showed a nitrogen peak not seen in the spectrum of the glassy area. This may be because most of the nitrogen is used up in the precipitation of $\text{Si}_2\text{N}_2\text{O}$ crystals, or perhaps because the nitrogen content of the glass area is small and thus below the EDS detectability limit.

4. Summary

Oxynitride glasses in Si-CaAlON and Si-CaAlBON systems were synthesized by conventional glass melting techniques. Si-CaAlON glasses were generally homogeneous but macroscopic inhomogeneous.

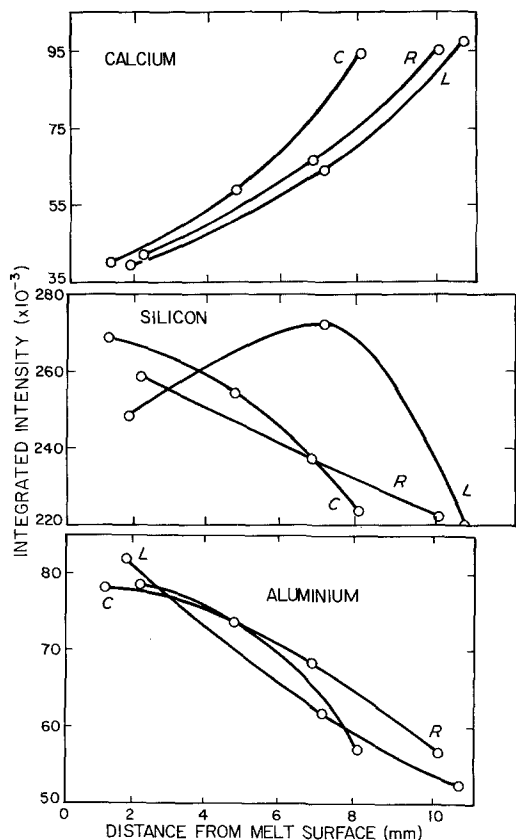


Figure 5 Integrated X-ray intensities of calcium, silicon and aluminium obtained from EDS spectra as a function of distance from the melt surface, *C* is the melt depth along the centre of the glass ingot, and *L* and *R* are distances from the surface along the left and right edges of the glass ingot shown in Fig. 3.

TABLE IV Summary of X-ray diffraction data on some heat treated (1350° C, 2 h) Si-Ca-Al-O-N and Si-Ca-Al, B-O-N glasses

Sample number*	Nitrogen content (at%)	X-ray identification of crystalline peaks
1	2	Unidentifiable phase(s)
2	6.5	Mixture of sillimanite and some other unidentifiable phase(s)
3	7.9	Amorphous pattern
4	8.5	Si ₂ ON ₂
5	11.2	Si ₂ ON ₂
8	3.1	α-cristobalite
9	7.0	Not sufficiently crystalline
10	8.0	Amorphous

*Refer to Tables I and II.

generity was observed in Si-CaAlBON glasses. The glass transition temperatures increased with nitrogen content as in other oxynitride glasses, and nitrogen-containing crystalline phases could be precipitated upon heat treatment of selected glasses.

Acknowledgement

This work is based on a MS thesis by Paul E. Jankowski and was supported by the US National Science Foundation under grant DMR 79-17660 administered by the Ceramics Program of the Division of Materials Research. The microscopy work was conducted in the Center for Microanalysis in the Materials Research Laboratory at Illinois.

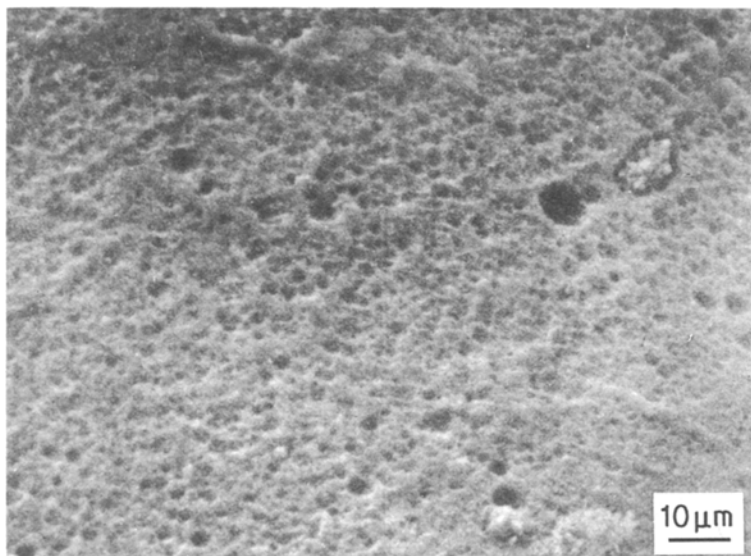


Figure 6 SEM micrograph of amorphous phase separation in a heat treated Si-CaAlON glass sample (Sample 3, Table I).

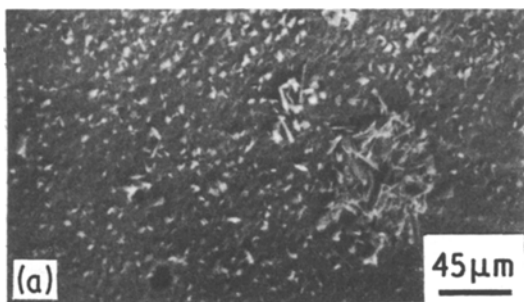
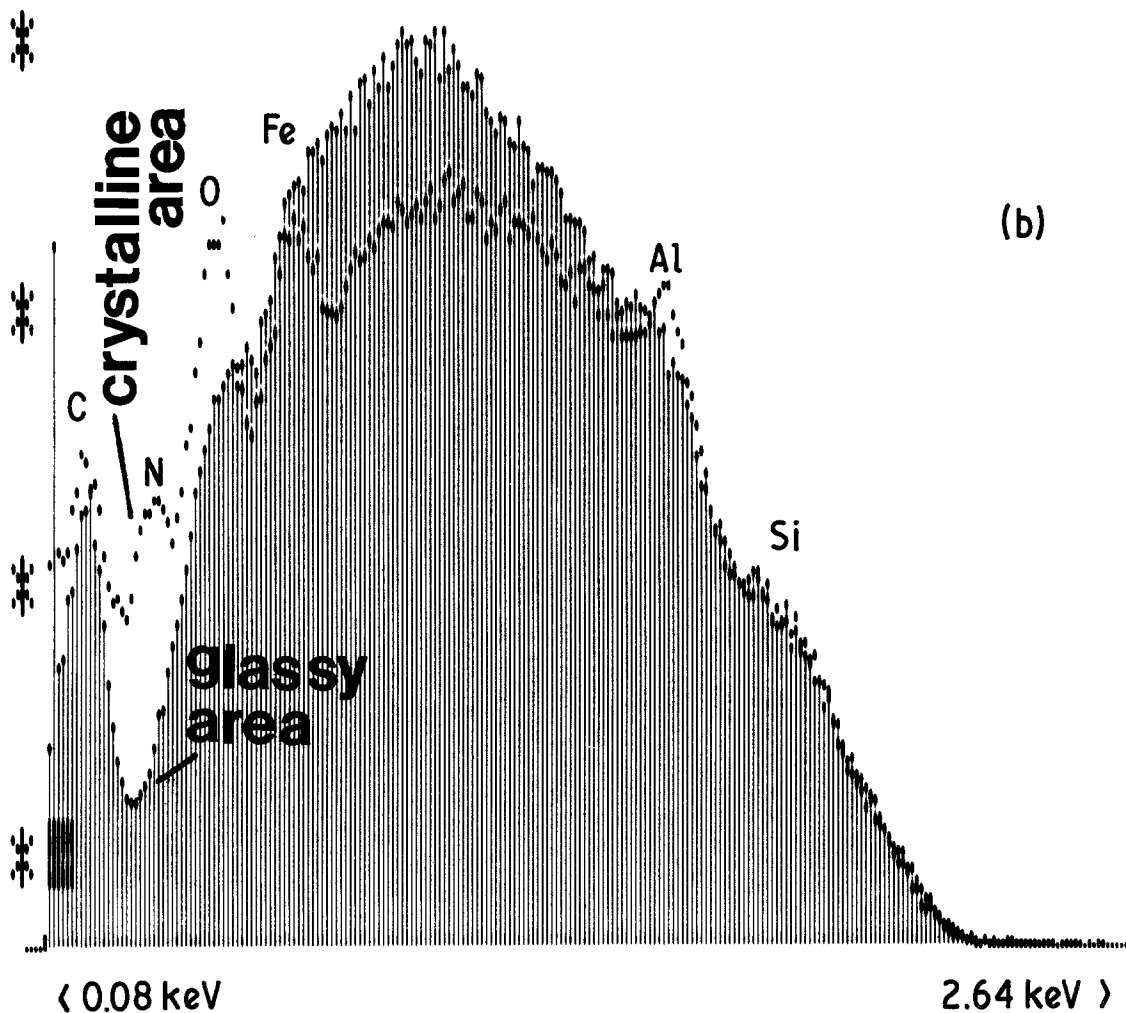


Figure 7 (a) SEM micrograph of a crystallized Si-CaAlON glass (Sample 4, Table I) showing crystals of $\text{Si}_2\text{N}_2\text{O}$ as identified by X-ray diffraction. (b) Energy dispersive X-ray spectrometry in a scanning auger microprobe reveals that the crystals in (a) contain nitrogen while the glassy area has no nitrogen peaks (glass may have a nitrogen content below the detectability limit of the instrument). Both the crystal and glass spectra show silicon, aluminium, and oxygen peaks in addition to carbon and iron peaks resulting from contamination.



References

1. H. O. MULFINGER, *J. Amer. Ceram. Soc.* 49 (1966) 462.
2. K. H. JACK, in "Nitrogen Ceramics", edited by F. L. Riley (Noordhoff International Publishing Co., Reading, Massachusetts, 1977).
3. K. CHYUNG and R. R. WUSIRIKA, US Patent No. 4141 739, Feb. 27, 1979; US Patent No. 4070 198, Jan. 24, 1978; US Patent No. 4097 295, June 27, 1978; US Patent No. 4186 021, Jan. 29, 1980; US Patent No. 4222 760, Sept. 16, 1980.
4. K. R. SHILLITO, R. R. WILLS and R. B. BENNETT, *J. Amer. Ceram. Soc.* 61 (1978) 537.
5. R. E. LOEHMAN, *ibid.* 62 (1979) 491.
6. *Idem*, *J. Non-Cryst. Solids* 42 (1980) 433.
7. P. E. JANKOWSKI and S. H. RISBUD, *J. Amer. Ceram. Soc.* 63 (1980) 350.
8. R. R. WUSIRIKA and C. K. CHYUNG, *J. Non-Cryst. Solids* 38-39 (1980) 39.
9. T. C. SHAW, PhD thesis, University of California-

- Berkeley (1980).
10. R. A. L. DREW, S. HAMPSHIRE and K. H. JACK, *Proc. Brit. Ceram. Soc., Special Ceramics 7* 31 (1981) 119.
 11. P. E. JANKOWSKI and S. H. RISBUD, *J. Amer. Ceram. Soc.* 65 (1982) C-29.
 12. D. R. MESSIER and A. BROX, *ibid.* 65 (1982) C-123.
 13. C. J. BRINKER, *Commun. Amer. Ceram. Soc.* 65 (1982) C-4.
 14. L. M. BAGAASEN and S. H. RISBUD, *Bull. Amer. Ceram. Soc.* 61 (1982) 368 (abstract only).
 15. W. K. TREDWAY and S. H. RISBUD, *J. Amer. Ceram. Soc.* 66 (1983) in press.

*Received 1 December
and accepted 13 December 1982*